

PARALLEL MAGNETIC RESONANCE IMAGING USING NEURAL NETWORKS

Neelam Sinha Manojkumar Saranathan K. R. Ramakrishnan

S. Suresh

Department of Electrical Engineering,
Indian Institute of Science,
Bangalore, India

School of EEE,
Nanyang Technological University,
Singapore

ABSTRACT

Magnetic resonance imaging of dynamic events such as cognitive tasks in the brain, requires high spatial and temporal resolution. In order to increase the resolution in both domains simultaneously, parallel imaging schemes have been in existence, where multiple receiver coils are used, each of which needs to acquire only a fraction of the total available signal. In our approach, we regularly undersample the signal at each of the receiver coils and the resulting aliased coil images are combined (unaliased) using the neural network framework. Data acquisition follows a variable-density sampling scheme, where lower frequencies are densely sampled, and the remaining signal is sparsely sampled. The low resolution images obtained using the densely sampled low frequencies are used to train the neural network. Reconstruction of the image is carried out by feeding the high-resolution aliased images to the trained network. The proposed approach has been applied to phantom as well as real brain MRI data sets, and results have been compared with the standard existing parallel imaging techniques. The proposed approach is found to perform better than the standard existing techniques.

Index Terms— Parallel Magnetic Resonance Imaging, undersampling, unaliasing, neural networks

1. INTRODUCTION

Magnetic Resonance Imaging (MRI) is a very popular medical imaging modality, due to its non-invasive nature and excellent soft-tissue contrast. MR signal acquisition occurs in the spatial-frequency domain (called k -space), of the object being scanned. The k -space samples are used to construct the image of the object. Spatial localization is achieved using magnetic field gradients applied in all three dimensions, which modulate the precession frequency of the protons as a function of space. The gradient along Z is called, slice selection, which determines the cross-section of interest. The gradients along Y and X , called phase and frequency encoding gradients, determine in-plane resolution and field of view. To create an MR image, we need to sample the two-dimensional k -space ($\Delta k_x, \Delta k_y$). Here, $\Delta k_x = \frac{\gamma}{2\pi} G_x \Delta t$ and $\Delta k_y = \frac{\gamma}{2\pi} G_y \tau_{pe}$, where γ is a constant associated with hydrogen protons, G_x is the frequency encoding gradient amplitude, Δt is the sampling period, G_y is the phase encoding gradient step size, and τ_{pe} is the phase encoding gradient duration.

In order to obtain an image with good spatial resolution, we need to acquire data farther out in k -space, implying larger number of phase encoding steps. However, an inherent limitation in MR imaging is that only one point in k -space can be acquired at any given instant of time. Hence, acquisition of more points would imply loss of resolution in time. Alternately, increasing Δk_y can reduce the number of phase encoding steps but at the cost of aliasing. This is the classic trade-off between spatial and temporal resolution in MRI,

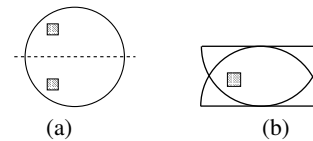


Fig. 1. Effect of downsampling (a) True image (b) Aliased image obtained by downsampling by 2

which is typically addressed using partial data reconstruction or parallel imaging techniques. Parallel imaging involves use of multiple receiver coils. Here, acceleration is achieved by regular undersampling and the resulting aliasing resolved by making use of redundant information collected from multiple parallel receivers. The final unaliased reconstructed images can be obtained by combining the signals either in image domain or in k -space. Existing techniques differ in aspects such as the domain they work in, the assumptions they make, and the nature of errors that they generate.

2. PARALLEL IMAGING

Parallel imaging was designed as a method to reduce the number of phase-encoding steps, the most time-expensive factor in MR Imaging. Here, multiple receiver coils are used in order to accelerate imaging. Each receiver coil is characterized by its spatial sensitivity function, which conveys information about the relative position of the origin of the received signal. Each coil provides the coil-weighted version of the image, all of which eventually can be combined to obtain the image reconstruction. It is well-established that if each of the receiver coils could acquire the entire k -space, then the best estimate of the true k -space would be the “sum of squares” (SoS). However, when the k -space at each of the receiver coils is sparsely sampled, then we need to devise ways to combine the acquired signals, in order to reconstruct the image. Methods like SENSE [1], SMASH [2], PILS [3], GRAPPA [4] are the known standard techniques used in parallel imaging.

2.1. Current techniques

SENSE combines the acquired signal in the image domain. Here, coil sensitivity information is used to combine the coil-weighted aliased images. Let us assume i_1 and i_2 to be the true intensities at the pixels shown in Fig.1(a). Let the coil sensitivities at those points be c_{11}, c_{12} and c_{21}, c_{22} for coils 1 and 2 respectively. The resulting intensity at the pixel marked in Fig.1(a), for coil 1 is say

α_1 , and for coil 2, α_2 . Then we know,

$$\begin{aligned} c_{11}i_1 + c_{21}i_2 &= \alpha_1 \\ c_{12}i_1 + c_{22}i_2 &= \alpha_2 \end{aligned}$$

The framework is represented as a linear system of equations will be over-determined, if the downsampling factor is less than number of receiver coils. SMASH is a k -space technique, where a composite k -space is generated using signals acquired in the array of receiver coils.

$$C^{total}(x, y) = \sum_j n_j C_j(x, y) \approx \exp^{i(m\Delta k_y y)} \quad (1)$$

where, n_j are complex weight factors, m is an integer, and Δk_y is the resolution along k_y . Here, the coils are designed such that the linear combinations of their acquisitions generate the missing harmonics. However, it turns out that the harmonic fit may not be exactly sinusoidal, leading to artifacts in reconstruction. GRAPPA is also a k -space technique, which again linearly combines the acquired lines to generate the missing lines. Here, a bunch of lines at the central k -space, called auto-calibration lines (ACS) are acquired along with the usual sparse acquisition. A ‘‘block’’ is defined as a single acquired line and $(A - 1)$ missing lines, where A is the downsampling factor.

$$S_j(k_y - m\Delta k_y) = \sum_{l=1}^L \sum_{b=0}^{N_b-1} n(j, b, l, m) S_l(k_y - bA\Delta k_y) \quad (2)$$

where $S_j(k_y)$ is the signal in coil j at line k_y , N_b is the number of blocks used in the reconstruction, l counts through the individual coils and b counts through the individual reconstruction blocks. The N_b lines which are separated by $A\Delta k_y$ are combined using the weights $n(j, b, l, m)$ to form each line, corresponding to a reduction factor A . This process is repeated for each coil in the array, resulting in L uncombined single coil images, which can be combined using the known optimal ways. A technique that works in image domain utilizing B -splines [5] for reconstruction in parallel imaging, was recently proposed. Here, coil-weighted aliased images are linearly combined to obtain the final image. The reconstruction operator is determined by using the low-resolution version of the signal. The same reconstruction operator is applied to the high-resolution version. The coefficients that linearly combine, are expressed as a linear combination of B -splines. The parameters are obtained by minimizing the error for the low-resolution acquisition.

In the proposed method, we make use of the above problem formulation, but solve it using neural network framework. In this approach, we do not need to make any assumptions of linearity or coil-sensitivities. An overview of the proposed system is shown in Fig.2. The rest of the paper is organized as follows. Section 3 explains the proposed approach. Section 4 discusses the data used and results. The conclusion of the paper is given in section 5.

3. PROPOSED APPROACH

In standard MRI, a single coil with homogeneous spatial sensitivity (body-coil) is used. The image (body-coil image) acquired this way serves as the benchmark to compare the reconstructed image using reduced data with parallel imaging schemes. The notations used here are taken from the paper [5]. The body-coil image is assumed to be the true image S . In parallel MRI, several receiver coils are used

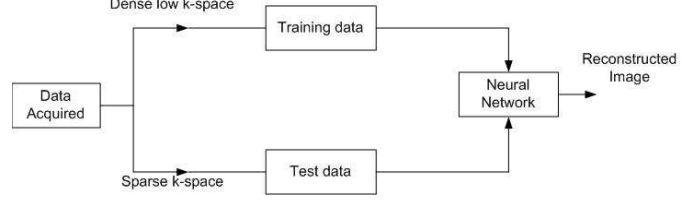


Fig. 2. Overview of the proposed method

simultaneously to acquire the signal. The image acquired from the l th coil, S_l is given as,

$$S_l(x, y) = C_l(x, y)S(x, y) \quad (3)$$

where C_l is the complex sensitivity of the l th coil.

It is well-known that sparse sampling in k -space causes aliasing in image domain. In the event of rectangular undersampling by factor M where N_y is the maximum number of phase encodes possible, the aliased image obtained at the l th coil, S_l^A is given by,

$$\begin{aligned} S_l^A(x, y) &= \sum_{m=0}^{M-1} S_l(x, y + m\frac{N_y}{M}) \\ &= \sum_{m=0}^{M-1} C_l(x, y + m\frac{N_y}{M})S(x, y + m\frac{N_y}{M}) \end{aligned} \quad (4)$$

where, $m = 0, 1, \dots, M - 1$. We assume the final reconstruction to be some arbitrary function \mathcal{F} of the aliased coil images. This is the function that we have set out to find. It must be noted that no assumptions are made about the nature of the function \mathcal{F} .

$$\hat{S}(x, y + m\frac{N_y}{M}) = \mathcal{F}(S_l^A(x, y)) \quad (5)$$

Constraining function \mathcal{F} in equation (3), given by

$$\mathcal{F}\left(S_l^A(x, y + m'\frac{N_y}{M})\right) = \begin{cases} \hat{S}(x, y + m\frac{N_y}{M}) & \text{for } m = m' \\ 0 & \text{for } m \neq m' \end{cases} \quad (6)$$

This forces the image to be split into as many blocks as the downsampling factor. This condition ensures that any reconstructed pixel from a given block, could only have been generated from pixels in the corresponding block from the coil-weighted aliased images. This condition is incorporated by designing as many neural networks as the undersampling factor.

3.1. Acquisition scheme

Full k -space 8-coil data was acquired for the experiments. Points from the acquired data were selectively chosen to form the testing and training data sets. A variable-density sampling scheme was chosen, as shown in Fig.3. The ‘‘sum of squares’’(SoS) image was assumed to be the gold standard image. The central k -space lines (32, in our experiments) were densely sampled at each of the receiver coils. The corresponding SoS reconstruction was the blurred unaliased image. The densely sampled lines were further subsampled to form the blurred, aliased coil images. The blurred aliased coil images along with the corresponding SoS image, form the training data set to the neural network. This data set establishes the functional



Fig. 3. Sampling scheme

relation between the aliased images and the corresponding unaliased version. The weights associated with the neural network topology are now determined. The trained neural network is now fed with full-resolution aliased coil images, to obtain the final image reconstruction.

3.2. Neural networks

Neural networks have emerged as a powerful mathematical tool for solving various problems like pattern classification, medical imaging due to their suitability for mapping complex characteristics, and learning. Of the many neural network architectures proposed, single hidden layer feed-forward network with sigmoidal or radial basis function are found to be effective for solving a number of real-world problems. The free parameters of the network are learned from the given training samples using gradient descent algorithm.

The architecture of the neural network used, comprises of an input layer, a hidden layer with 98 neurons and an output layer. The input features are 18-dimensional, of which 16 are derived from the complex intensities of the 8 (split complex numbers as real, imaginary) aliased coil images. The remaining 2 components are used to index the position of the pixel. Each pixel position of the aliased images represents a feature vector.

3.3. Validation criterion

Errors in image reconstruction are quantified using error images, with indices like PSNR and a similarity index to compare the closeness of the reconstructed image against the original image, called “Structural Similarity” index (SSIM) [6]. This index penalizes loss in structural correlation, intensity and contrast. This is a well-known Full-Reference image quality metric, widely used to quantify image quality, given a reference image and its distorted version.

4. RESULTS

4.1. Phantom data

The proposed technique was applied to the standard “Shepp-Logan” phantom. Three separate cases, the standard phantom, Phantom corrupted with complex additive Gaussian noise and Phantom with a fine grid-structure super-imposed were studied. The distinct structures in the phantom reconstruction are separately assessed. A comparison of the SSIM indices obtained using the proposed method, as well as the standard existing techniques, is as shown in table1, all of which are carried out for downsampling factor of 4. The comparison of the SSIM indices for the noisy-phantom case is shown in table 2. A grid of varying thickness and intensities, spread out, was superimposed on the phantom to determine the abilities of the techniques to reproduce fine structures. The comparison of PSNR between the techniques is shown in table.4. It can be seen that PSNR obtained using the proposed approach and GRAPPA are quite comparable, while that obtained using SENSE is far below them both,

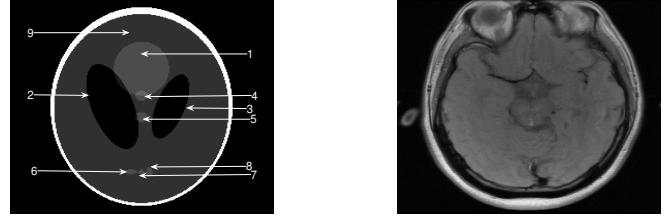


Fig. 4. Original Image (color scale : 0 to 1) (a)Phantom (b) Real MR structural brain

Table 1. Comparison of SSIM Indices for distinct regions of the phantom

Region	Proposed	GRAPPA	SENSE
1	0.8919	0.6693	0.4647
2	0.5237	0.3954	0.5468
3	0.5866	0.4055	0.7406
4	0.9443	0.1320	0.3883
5	0.8919	0.6693	0.4647
6	0.9912	0.6683	0.3871
7	0.3902	0.8369	0.1914
8	0.7378	0.6692	0.3212
9	0.7780	0.6682	0.4781

especially in the noisy case since SENSE performs best only under ideal conditions. However, when visually assessed it can be seen that the reconstruction obtained using the proposed technique, is better. The nature of errors of the proposed method depends on the spatial location, spread and intensities, as shown by the poor performance on region 7, which is a small low-intensity oval region squeezed between two similar regions (see Fig. 4(a)).

4.2. Real data

The proposed approach was applied on real data sets of brain MR images. 4 volumes of fmr data sets, and the structural brain data set (8-coil data) available on [7], were utilized. All simulations were carried out in matlab. The data matrix was of size 256×256 . The central 32 lines were densely sampled, while the remaining k -space was sparsely sampled, depending on the downsampling factor. Figure 5 shows comparison of reconstruction for downsampling factor of 4, for the structural brain image shown in Fig. 4(b). The same sparsely sampled data was used for reconstruction using the standard existing parallel imaging techniques, SENSE and GRAPPA, for downsampling by 4 and 32 densely sampled low k -space lines.

The comparison between error images shows that errors obtained using SENSE and GRAPPA reconstruction, are more than that obtained using the proposed approach. While errors in GRAPPA reconstruction are spread out, errors in SENSE reconstructions are localized. The proposed method results in errors resembling GRAPPA. In terms of PSNR, the proposed approach gives a gain in PSNR of 10dB over SENSE, while it is comparable with that obtained using GRAPPA.

Table 2. Comparison of SSIM Indices for distinct regions of the phantom, corrupted with noise

Region	Proposed	GRAPPA	SENSE
1	0.8025	0.6735	0.4633
2	0.5526	0.4811	0.5895
3	0.6254	0.5111	0.7670
4	0.8433	0.1403	0.3920
5	0.9340	0.6721	0.3860
6	0.8089	0.7808	0.3164
7	0.2757	0.8366	0.1825
8	0.6642	0.6721	0.3176
9	0.7293	0.6905	0.4846

Table 3. Comparison of SSIM Indices for distinct regions of the phantom, with grid super-imposed

Region	Proposed	GRAPPA	SENSE
1	0.7919	0.5664	0.4003
2	0.5612	0.3620	0.4586
3	0.6230	0.4366	0.5778
4	0.8822	0.0558	0.3687
5	0.9163	0.5980	0.3631
6	0.8127	0.6256	0.2727
7	0.3705	0.7663	0.2186
8	0.6603	0.5225	0.3258
9	0.7211	0.5849	0.4242

5. CONCLUSION

In this paper, we have proposed a method to reconstruct images for parallel magnetic resonance imaging, in neural network framework. Variable density data acquisition is carried out at all the receiver coils. Low frequencies are densely sampled while the remaining frequencies are sparsely sampled. Low frequency data serve to train the network to determine the associated weights. This approach was tested on phantom as well as real brain MR images and compared with the standard existing parallel imaging techniques. Results were evaluated using criteria like PSNR and Structural similarity index.

6. REFERENCES

- [1] K. P. Pruessmann, M. Weiger, M. B. Scheidegger, and P. Boesiger, "Sense : Sensitivity encoding for fast mri," *Magnetic Resonance in Medicine*, vol. 42, no. 5, pp. 952–962, 1999.
- [2] D. K. Sodickson and W. J. Manning, "Simultaneous acquisition of spatial harmonics (smash): ultra-fast imaging with radio frequency coil arrays," *Magnetic Resonance in Medicine*, vol. 38, no. 4, pp. 591–603, 1997.
- [3] M. A. Griswold, P.M. Jakob, R. M. Hedemann, and A. Haase, "Parallel imaging with localized sensitivities (pils)," *Magnetic Resonance in Medicine*, vol. 44, no. 4, pp. 602–609, 2000.
- [4] M. A. Griswold, P. M. Jakob, R. M. Hedemann, M. Nittka, V. Jellus, J. Wang, B. Keifer, and A. Haase, "Generalized au-

Table 4. Comparison of PSNR

Phantom	Proposed	GRAPPA	SENSE
Noise-less	26.6428	27.3008	14.7836
Noisy	24.9667	27.3636	6.9231
With Grid	25.1871	25.0629	15.3063

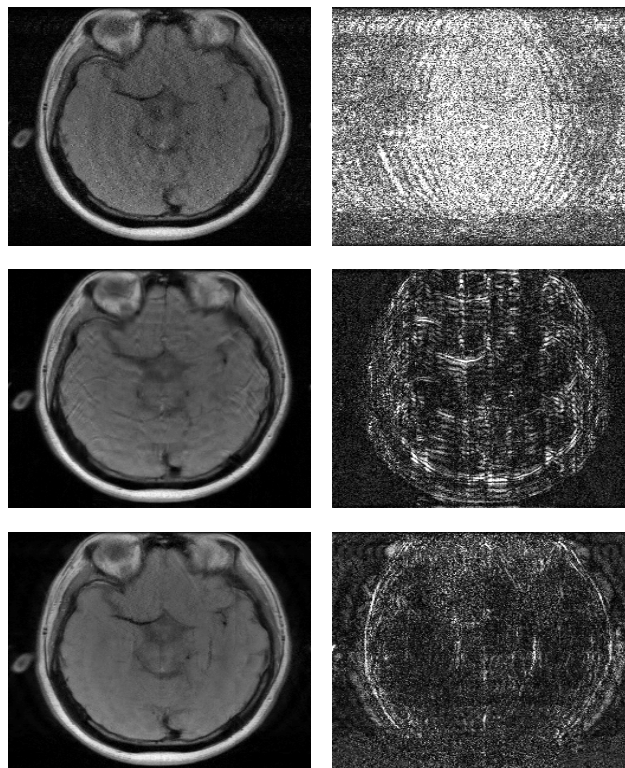


Fig. 5. Left column : Reconstruction Comparison (Top : SENSE, Middle : GRAPPA , Bottom : Proposed method (color scale : 0 to 1) Right column : Corresponding errors (color scale : 0 to 0.16)

localizing partially parallel acquisitions (grappa)," *Magnetic Resonance in Medicine*, vol. 47, no. 6, pp. 1202–1210, 2002.

- [5] Jan Petr, Jan Kybic, Sven Muller, Vaclav Hlavac, and Michael Bock, "Parallel mri reconstruction using b-spline approximation," *Proceedings of 13th ISMRM*, pp. 2421–2421, 2005.
- [6] Z. Wang, A. C. Bovik, H. R. Sheikh, and E. P. Simoncelli, "Image quality assessment: From error measurement to structural similarity," *IEEE Transactions on Image Processing*, vol. 13, no. 4, pp. 600–612, Apr. 2004.
- [7] PULSAR: Parallel-Imaging Utilizing Localized Surface-coil Acquisition and Reconstruction, "http://www.ece.tamu.edu/~mrsl/JIMJI_TAMU/pulsarweb/"